Theory and Practice of Science and Technology
2025, VOL. 6, NO. 7, 124-132
DOI: 10.47297/taposatWSP2633-456925.20250607

Optimisation of Control Algorithms for Bionic Ray Squid Robot

Yuhan Sun*

Faculty of Electrical and Control Engineering, Liaoning Technical University, Huludao, Liaoning, 123032, China

ABSTRACT

In recent years, the demand for ocean exploration and the urgency of national security needs have driven the rapid development of bionic robotics. Underwater bionic robot is becoming an important direction in the field of ocean exploration, ecological monitoring and military reconnaissance. In this paper, based on the characteristics of the ray's flat body and wave-like swimming mode, we design the bionic ray robot, and combine the traditional PID control with the fuzzy algorithm to form the fuzzy adaptive PID control, which can significantly improve the control performance of the system under the nonlinear, time-varying and uncertain environment. The simulation test results show that compared with the traditional PID control of the bionic ray robot, its underwater operation capability is significantly improved by using fuzzy adaptive PID; it has higher operational flexibility and can complete the exploration tasks more efficiently, which has important research value and application prospects.

KEYWORDS

Bionic skate; Fuzzy adaptive PID; Flexibility; Exploration tasks

I Introduction

In recent years, soft robots have received widespread attention. Compared with traditional rigid robots, soft robots, with their highly flexible and adaptable features, have shown great potential in the fields of medical care, ocean exploration, industrial automation and so on. At the same time, bionic robots have also become one of the important directions in robotics research. By imitating the movement, structural characteristics and behavioural patterns of natural organisms, bionic robots are able to demonstrate superior mobility and energy efficiency in complex environments.

Further in the field of underwater robotics, the traditional propulsion method mainly relies on propellers and jet propellers, which have certain advantages in speed and thrust, but still have limitations in manoeuvrability, energy-efficiency ratio and eco-friendliness in complex underwater environments. Therefore, biomimetic propulsion technology based on fish, marine mollusks and other organisms has become a popular direction for underwater robotics research. Many scholars at home and abroad have conducted extensive research on this literature review. Shen Yan et al. designed an underwater bionic flapping robot by imitating the swimming mode of sea turtles and adopting the principle of limb structure of sea turtles, which can quickly and accurately obtain the information of the ship's hull, achieve the all-round monitoring and detection of the ship's hull, and improve the detection efficiency and recognition accuracy [1]; Ding Lehan et al. developed a new bionic herding and fishing robot suitable for a variety of environments, and established a mathematical model and kinematic model of the 12 rudders jointly driving the bionic fins of the fish. mathematical model and kinematic model of the bionic fins, and proposed an optimal design scheme of the propulsion mechanism, which makes the bionic herding and fishing robot have a higher efficiency compared with the traditional underwater robots [2]; Since the fluctuation propulsion of aquatic organisms such as the nigger swordfish has a high degree of manoeuvrability and stability of the movement, the study introduces a synergistic propulsion system combining hydrofoils and wave fins to improve the propulsive performance by studying their interactions in various motion modes [3]; Ding Han et al. interactions to improve the propulsion performance [4]; Yuan-Jie Chen et al. proposed a new kinematic model aimed at overcoming the difficulties caused by the current lack of understanding of the pectoral fin structure and the restricted range of pectoral fin motion in traditional research methods, which provides valuable guidance for the design of bionic pectoral fins and thus enhances the application of the bionic bullnose ray robots [5]; Xinii Zhou et al. presented the a design solution for a bionic robotic fish with an integrated tail and pectoral fin structure, which provides greater flexibility and higher propulsion efficiency than traditional propeller-driven vehicles [6]. However, there are fewer studies on ray bionic robots, and the existing ray bionic robots have poor compliance in the fluid environment, which is difficult to realistically reproduce the natural fluctuations of the ray and the motion control methods mostly use open-loop control or feedback control based on simple PID, which makes it difficult to adaptively adjust the motion mode in complex underwater environments, based on which this paper designs a ray bionic robot structure, and the kinematic model establishment is carried out for the fin section. The kinematic modelling is carried out, and finally the fuzzy control optimization PID algorithm is used to achieve the precise regulation of fin motion and improve the motion ability and environmental adaptability. Compared with the traditional PID in the face of perturbation, speed change, response speed

*** Corresponding Author:** Yuhan Sun, lmuria@163.com.

is improved.

2 Bionic ray model design and feasibility analysis

2.1 3D model design of bionic ray robot

The ray is recognisable among marine life by its unique body structure. Its wide pectoral fins spread out in a wing-like pattern, allowing it to move through the water as if it were "flying". In addition, the ray has an elongated tail fin with a sharp end, which not only helps to maintain its posture and balance, but also serves as an effective attack tool during feeding. The swimming mechanism of rays is largely dependent on their flat body structure and the way their pectoral fins fluctuate. As a cartilaginous fish, rays propel themselves by waving the edges of their pectoral fins, and are particularly adept at semi-buried dives in seafloor sediments. This special movement pattern not only enhances its stealthiness, but also its ability to manoeuvre in complex terrain. In this paper, based on the biological characteristics of the ray in terms of morphology, locomotion mode and stealth performance, a biomimetic ray robot scheme is designed and proposed, and its three-dimensional structural model is established using SolidWorks software, as shown in Fig.

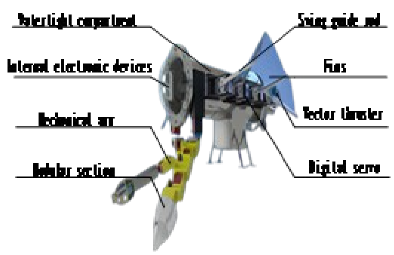

Figure 1 Schematic diagram of the structure of the bionic ray robot

As shown in the figure, the main body of the bionic ray robot consists of a watertight chamber, an oscillating guide rod mechanism and its drive, fins and vector thrusters. Its mechanical structure adopts a modular design to achieve functional diversity and flexible system configuration. During underwater operation, the robot is equipped with two propulsion modes: the fins are driven by the oscillating guide rod mechanism to generate fluctuations to achieve bionic propulsion when it is close to the pipe wall, working on the seabed, or when it needs to change direction quickly; and the vector thruster provides stable and strong power when it needs to move forward at high speeds or when it needs to cope with turbulent environments. The modular design of the end of the arm allows it to flexibly replace tools according to operational requirements, thus adapting to changing underwater operational scenarios and significantly improving task execution efficiency and operational flexibility. For different objects, the operator end can be equipped with different types of detachable mechanical claws to complete the tasks of grasping, operation or detection. In summary, the main structure of the bionic ray robot provides stable forward power, the vector propulsion system is used to achieve acceleration and direction adjustment, and the modular robotic arm is responsible for specific underwater operation functions. The arm is connected to the main structure through the bolt holes on the side of the watertight compartment, and the vector propulsion system is used to control the propulsion direction through the expansion and contraction of the cardan shaft and the directional rod.

2.2 Mathematical modelling

It is found that the ray mainly uses its wide pectoral fins to generate fluctuations to propel forward when it moves smoothly, so the focus of this paper is to analyse the principle of the pectoral fins generating fluctuations to make it propel forward and construct a mathematical model. The ray's pectoral fins generate fluctuating deformations through regular muscle contractions, which interact with the water to achieve propulsion. Specifically, rays swim by moving their large, flattened pectoral fins to create a wave that pushes the surrounding water backwards, and due to conservation of momentum, the fish is pushed forward. A mathematical model is constructed through the principle of fluctuation in the pectoral fins of a ray.

The fluctuation shape equation is first established:

The fin motion of a ray can be approximated as a sinusoidal wave propagation, defining the fluctuating form equation of the fin;

The gradual change in wave amplitude from root to inter-fin can be modelled using a Gaussian function.

$$y(x,t)=A(x)\sin(kx-wt+\varphi)$$
$$A(x)=A_0e^{-\alpha x} \quad (1)$$

From (1):

$$y(x,t)=A_0e^{-\alpha x}\sin(kx-\omega t+\varphi) \quad (2)$$

Where: y(x,t) : vertical displacement of a point at time t; x : length coordinate of the fin; A_0 : maximum amplitude; α : attenuation coefficient; $k=\frac{2\pi}{\lambda}$: wave number

From the equation, it is evident that the numerical variation along the y-axis resulting from the sinusoidal deformation of the pectoral fin is solely dependent on the wave frequency, amplitude, and wavelength. Altering any one of these three parameters will lead to a distortion in the sinusoidal wave produced during the motion of the robot's pectoral fin. By determining the maximum point attainable by the robot's pectoral fin, which corresponds to the wave amplitude, the change in the y-direction can be calculated.

Next establish the velocity and acceleration equations:

The velocity and acceleration at a point on the fins can be obtained by taking the partial derivatives from $y(x,t)$ to find the transverse velocity, i.e., the fluctuating square

Directional and lateral acceleration and flow velocity over the fins (local velocity field):

$$v_y=\frac{\partial y}{\partial t}=-\omega A_0e^{-\alpha x}\cos(kx-\omega t+\varphi)$$
$$a_y=\frac{\partial^2 y}{\partial t^2}=-\omega^2 A_0e^{-\alpha x}\sin(kx-\omega t+\varphi) \quad (3)$$
$$v=(U,v_y)$$

where U is the overall forward velocity of the fish and v_y is the local fluctuation velocity of the fins;

Oscillatory propulsion modelling is then performed to model simple harmonic motion:

$$\theta(t)=\theta_0\sin(\omega t+\varphi) \quad (4)$$

Where: θ(t) is the fin swing velocity relative to the fish body, and θ_0 is the maximum swing angle;

Solving for the end velocity of a fin can be done using the angular velocity formula:

$$v=r\frac{d\theta}{dt}=r\omega\cos(\omega t+\varphi) \quad (5)$$

where r is the length of the fin.

The hydrodynamic equation is:

$$F=\frac{1}{2}C_L\rho v^2S \quad (6)$$

where C_L is the lift coefficient, ρ is the density of the water, v is the local velocity of the fin, and S is the projected area of the fin.

Finally for propulsion calculations, the static thrust of the bionic ray propulsion is calculated:

$$F_x=\rho\int_0^L(-\frac{\partial y}{\partial t}\frac{\partial y}{\partial x})dx \quad (7)$$

Where: F_x is the propulsive force, the equation shows that the propulsive force is determined by the propagation of the fluctuations on the fins and the interaction of the water.

2.2.1 Feasibility analysis of watertight compartments

The watertight compartment mainly undertakes the following three functions. The first is the sealing and protection function, which needs to ensure good sealing performance during the design process to prevent key components from failing due to water ingress. Second is the pressure-resistant structure design, through the selection of high-strength materials and the use of cylindrical and other optimised structural forms, in order to enhance its ability to resist deep water and high pressure, to prevent deformation or rupture of the cabin under high-pressure environments. In addition, the pressure compensation function is also required to reduce the load on the sealing system by introducing a pressure compensation mechanism, so as to enhance its stability and reliability in long-term deep-sea operations. At the same time, in order to improve the system integration and adaptability, the structural design of the watertight module also needs to consider the functional modularity and the adaptability of the bionic motion system.

Most of the common watertight chamber structures on the market today are of traditional cylindrical design. In this paper, a pressure simulation analysis of the structure was carried out with a water depth of 40 metres (corresponding to about 5 atmospheres, 0.506625 MPa) as the working condition. The simulation results show that the water pressure is mainly concentrated in the bottom area of the watertight compartment, which is easy to lead to a large stress concentration in this area, thus triggering structural damage or even rupture. For this reason, this paper optimises the design of the bottom structure of the watertight compartment so that it can disperse the external water pressure more uniformly, thus effectively improving the pressure resistance and service life of the overall structure. The optimisation effect is shown in Fig.

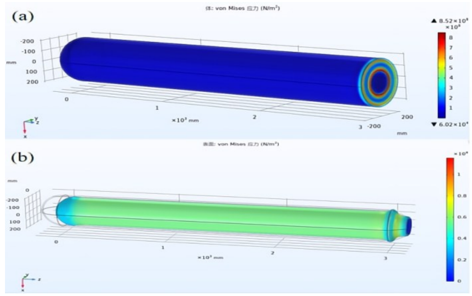

Figure 2 Simulation analysis of watertight compartment pressure

2.2.2 Kinematic simulation analysis of the fin mechanism

The ray's pectoral fins are fused with its head to form a flat fan-shaped structure, which generates propulsion through wave-like oscillations, and this type of motion is suitable for long and slow cruising on the seabed; the flexible oscillations of its pectoral fins can reduce the disturbance of water currents; and its wide pectoral fins can move independently or in concert, which allows the ray to adjust its direction, stop sharply, or raise and lower vertically in a quick manner. We designed a 3D model of the fin mechanism according to the characteristics of the ray, as shown in Fig. Multiple rudders are distributed along the axial direction of the fins to drive the remote linkage flexible fin surfaces, which are segmented to generate phase-difference oscillations to simulate the wave-like motion of the fins, and springs or elastic hinges are added between the oscillating remote rods and the fin surfaces to enhance the continuity and adaptability of the motion as shown in Fig.

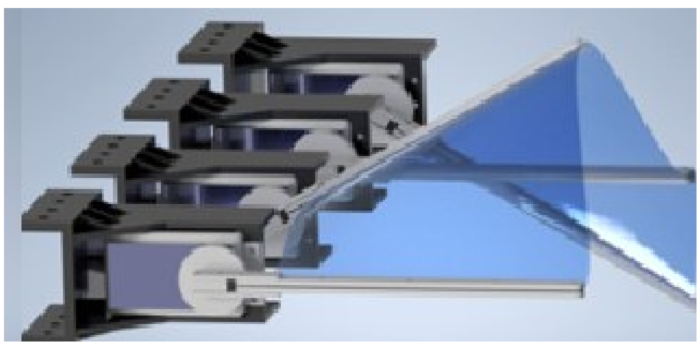

Figure 3 3D model of the fin mechanism

The flow velocity diagrams of the surrounding fluid affected by the fin motion at fin angles of 30° and -30° are analysed by fin simulation in COMSOL as shown in Fig.

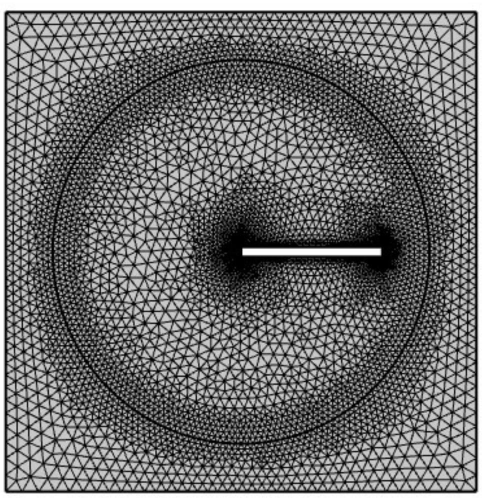

Figure 4 Structure of fins in COMSOL

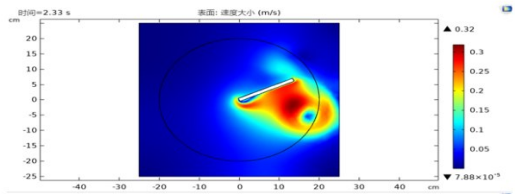

Figure 6 Fin angle of 30 degree

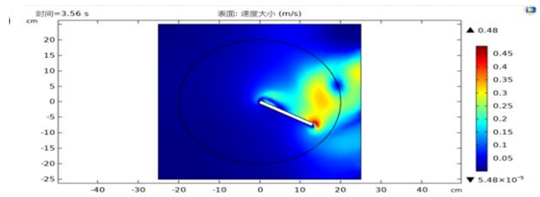

Figure 6 a.Flow velocity of fluid around fin angle

3 Optimised pid algorithm for fuzzy control

Because of its fluctuating propulsion mechanism and multi-degree-of-freedom motion characteristics, the bionic ray robot has extremely high requirements on the dynamic response, anti-interference ability and nonlinear adaptability of the control system. Although the traditional PID control has a simple structure, it is prone to overshooting and steady state error in complex underwater environments, and the optimisation of the PID parameters by combining with the fuzzy control can significantly improve the robustness of the system. Fuzzy PID control takes the deviation e and the change ec of deviation as inputs, and uses fuzzy control rules to adjust the PID parameters online to meet the different requirements of the PID parameters for different deviations e and increments ec of deviation. Its structure diagram is as follows:

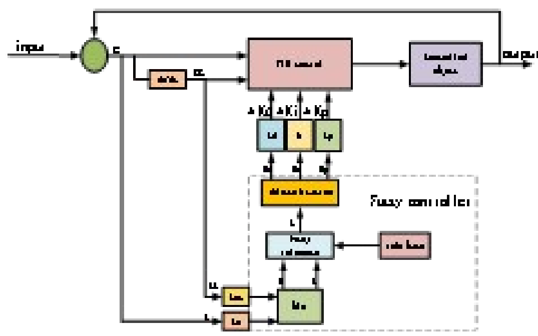

Figure 7 Fuzzy control PID structure

3.1 Fuzzy PID function

The formula for fuzzy PID is as follows:

$$K_e = N_e / a_e \tag{8}$$

$$K_{ec} = N_{ec} / a_{ec} \tag{9}$$

$$K_p = K_{p0} + \Delta K_p \tag{10}$$

$$K_i = K_{i0} + \Delta K_i \tag{11}$$

$$K_d = K_{d0} + \Delta K_d \tag{12}$$

3.2 Design of fuzzy rules

Firstly, e and ec are fuzzified to obtain the input fuzzy variables E and Ec; the input fuzzy variables E and Ec are divided into seven fuzzy subsets, i.e., {NB, NM, NS, ZO, PS, PM, PB}, which stand for negative large, negative medium, negative small, zero, positive small, positive medium, and positive large, respectively. Then the fuzzy rule base is established based on the fuzzy sets. As shown in Fig.

Table 1 Kp fuzzy rule design

E	EC						
	NB	NM	NS	Z	PS	PM	PB
NB	PB	PB	PM	PM	PS	Z	Z
NM	PB	PB	PM	PS	PS	Z	NS
NS	PM	PM	PM	PS	Z	NS	NS
Z	PM	PM	PS	Z	NS	NM	NM
PS	PS	PS	Z	NS	NS	NM	NM
PM	PS	Z	NS	NM	NM	NM	NB
PB	Z	Z	NM	NM	NM	NB	NB

Table 2 Ki fuzzy rule design

E	EC						
	NB	NM	NS	Z	PS	PM	PB
NB	NB	NB	NM	NM	NS	Z	Z
NM	NB	NB	NM	NS	NS	Z	Z
NS	NB	NM	NS	NS	Z	PS	PS
Z	NM	NM	NS	Z	PS	PM	PM
PS	NM	NS	Z	PS	PS	PM	PB
PM	Z	Z	PS	PS	PM	PB	PB
PB	Z	Z	PS	PM	PM	PB	PB

Table 3 Kd fuzzy rule design

E	EC						
	NB	NM	NS	Z	PS	PM	PB
NB	PS	NS	NB	NB	NB	NM	PS
NM	PS	NS	NB	NM	NM	NS	Z
NS	Z	NS	NM	NM	NS	NS	Z
Z	Z	NS	NS	NS	NS	NS	Z
PS	Z	Z	Z	Z	Z	Z	Z
PM	PB	PS	PS	PS	PS	PS	PB
PB	PB	PM	PM	PM	PS	PS	PB

3.3 Anti-fuzzification

According to the fuzzy design rule table of Kp, Ki, Kd, 49 fuzzy rules are designed to design the fuzzy controller and the fuzzy rules are established as shown in Fig:

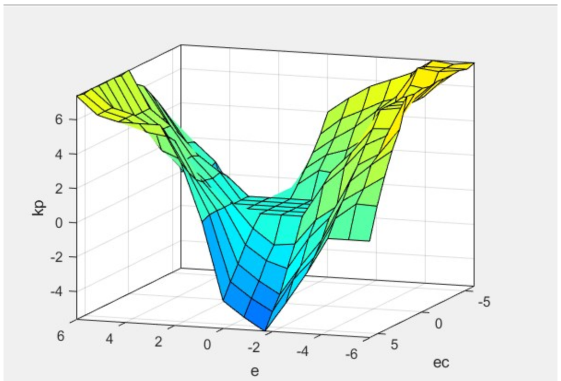

Figure 8 Kp

The tail of the ray squid underwater bionic robot uses an appropriate amount of propulsion, which aims to make the bionic robot move forward quickly underwater. The underwater propulsion motors are mainly permanent magnet motors (PM motors), including permanent magnet DC motors, brushless DC motors, and permanent magnet synchronous motors (PMSMs), which exhibit high power density and high efficiency by virtue of their permanent magnet excitation characteristics. The brush structure, weak magnetic structure and the use of sinusoidal current drive of permanent magnet synchronous motors are more suitable for underwater operation than the first two, therefore, permanent magnet synchronous propulsion motors become a more suitable choice for those occasions where there are strict requirements on underwater noise and weak magnetic range.

The simulation model was built by simulink to optimise the controller of the bionic robot by comparing the traditional PID controller with the fuzzified PID controller as shown in Fig.

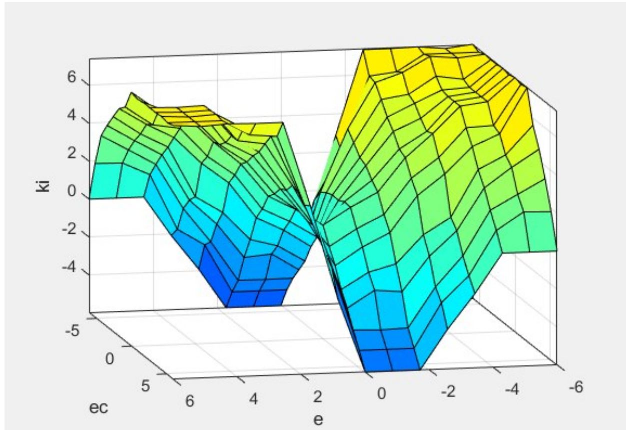

Figure 9 Ki

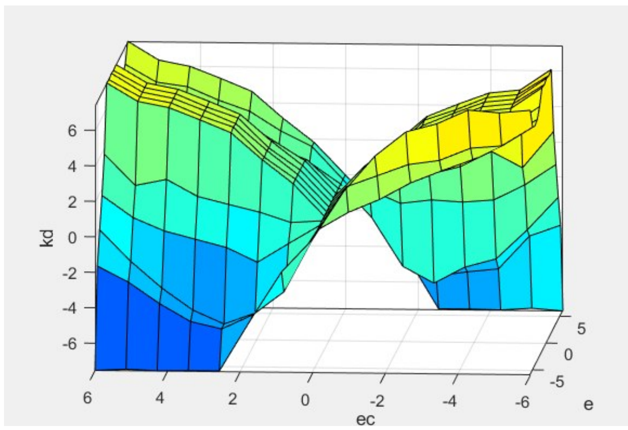

Figure 10 Kd

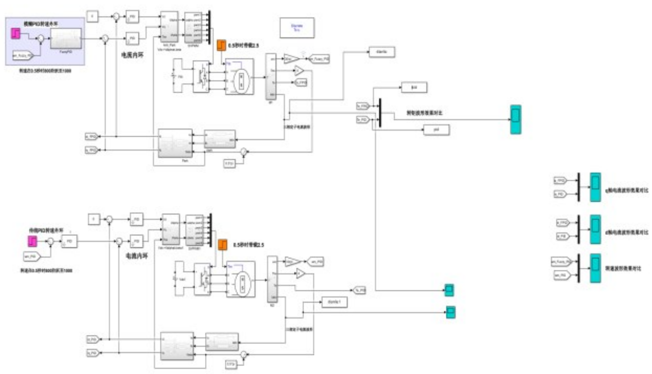

Figure 11 Simulation model of permanent magnet synchronous motor

During the motor starting process, it is divided into three stages:

The First stage is the current rise stage. When $I_d \geq I_{dl}$, the motor starts to start. Due to the electromechanical inertia effect, the speed does not increase rapidly. Therefore, the input deviation voltage of the speed regulator ASR is still large, and its output voltage remains at the limit value, forcing the current to rise rapidly.

The second stage is the constant current speed-up stage.ASR remains saturated, and the speed loop is equivalent to an open loop. The system becomes a current regulation system with a constant current given, basically maintaining the current constant. Therefore, the system's acceleration is constant, and the speed increases linearly.

The third stage is the speed regulation stage.When the speed rises to the given value, the input deviation of the speed regulator ASR reduces to zero, but its output remains at the limit value due to the integral action, so the motor is still accelerating, causing the speed to overshoot. As long as it is still greater than the load current, the speed continues to rise. Until $I_d = I_{dl}$, the torque $T_e = T_L$, the speed n reaches its peak. After that, the motor begins to decelerate under the resistance of the load.

After running this simulation model, the current diagram of Fuzzy PID, current diagram of PID and torque diagram of Fuzzy PID are obtained as shown below.

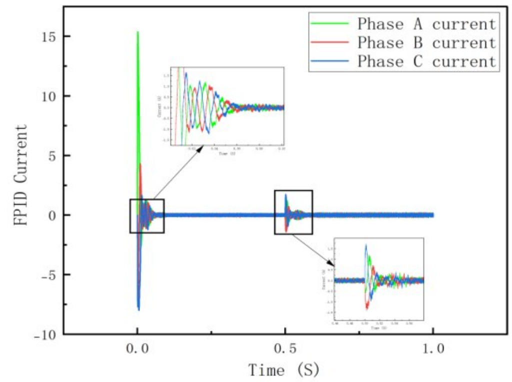

Figure 12 The current diagram of Fuzzy PID

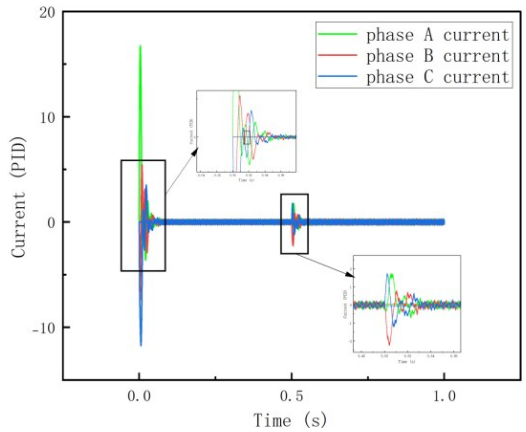

Figure 13 Current diagram of PID

This can be seen from the two three-phase current waveforms:

When PID is the controller, the peak values of three-phase current oscillations are 16.73A, 5.46A, 11.6A at the beginning of simulation, and the adjustment time is about 0.08s; the peak values of three-phase current oscillations after adding perturbation are 1.73A, 2.18A, 1.76A, and the adjustment time is about 0.54s. When fuzzy PID is the controller, the peak values of three-phase current oscillations are 15.29A, 4.27A, 8A, and the adjustment time is about 0.06s; the peak values of three-phase current oscillations after adding perturbation are 1.11A, 1.22A, 1.1A, and the adjustment time is about 0.06s. 15.29,A 4.27A, 8A,the regulation time is about 0.06s; after adding the perturbation, the oscillation peaks of the three-phase current are 1.11A, 1.22A, 1.63A in order, and the regulation time is about 0.52s. It can be seen that the fuzzy PID can effectively improve the oscillation time and regulation time, and make the system more stable.

Comparing the effect of fuzzy PID and PID controllers on speed is shown in Fig.

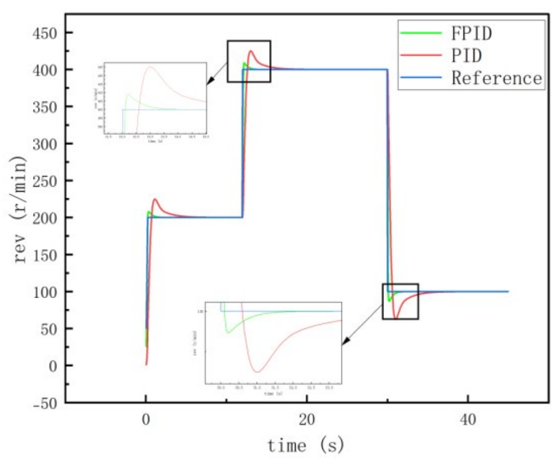

Figure 14 Torque diagram

The simulation starts running, when the permanent magnet synchronous motor is in the current rising stage: the overshooting amount of the fuzzy PID is 4%, and the regulation time is 2.15s; the overshooting amount of the PID is 12.5%, and the regulation time is 8.8s. When the permanent magnet synchronous motor is in the constant current speed rising stage: the overshooting amount of the fuzzy PID is 2.25%, and the regulation time is 14.25s; the overshooting amount of the PID is 6.25%, and the regulation time is 21.5s. When the permanent magnet synchronous motor is in the deceleration stage: the overshooting amount of fuzzy PID is 13%, and the regulation time is 32.55s; the overshooting amount of PID is 37.3%, and the regulation time is 37.45s. It can be seen that, compared with the traditional PID control, the overshooting amount of fuzzy PID for the startup of the permanent magnet synchronous motor is obviously reduced, and the regulation time is also faster.

References

[1] SHEN Yan, LIU Tianxun, JIA Binbin. Design and analysis of bionic flapping wing robot for underwater hull detection [J]. Ship Science and Technology, 2024, 46 (23): 111-115.

[2] MO Xiong,YAN Fulin,WEN Yi,ZHOU Dongdong Optimization of synchronous control performance of ship lock herringbone gate based on PID algorithm[J]. Mechanical and Electrical Information, 2025, (9): 43-46.

[3] ZHOU Xing,WU Tianchen,YANG Fan,LI Wenyang,LIU Jia,WANG Yuqiang Design and simulation of biomimetic ray robot[J]. Robot Technology and Applications, 2025, (1): 27-31.

[4] Yiting Liang, Jian Wang, Debiao Lu, Jiang Liu, Baigen Cai. Train Convoy Headway Optimization Method Based on Variable Domain Fuzzy PID Control Algorithm[OL]. https://doi.org/10.1007/s40815-025-02030-z.Int. J. Fuzzy Syst. 2025.

[5] Yuanyuan Wu, Renjie Fu, Junfeng Zhang, Bhatti Uzair Aslam. Practical PID Protocol of T−S Fuzzy Positive Multi-Agent Systems Under Attacks [OL].https://doi.org/10.1007/s40815-025-02002-3. Int. J. Fuzzy Syst. 2025.

[6] Eroğlu Murat, Şam Parmak Ebru Devrim. A simple manufacturing process of the miniaturised octopus-inspired underwater soft robotic grippers[J]. Journal of Adhesion Science and Technology, 2023, 37 (7).